Sławomir WOŚ[*], Waldemar KOSZELA[*], Paweł PAWLUS[*]

THE EFFECT OF OIL POCKET ARRAYS ON FRICTION COEFFICIENT

WPŁYW SZYKU KIESZENI SMAROWYCH NA WSPÓŁCZYNNIK TARCIA

Key words:	textured surfaces, pin-on-disc, friction force, abrasive jet machining.
Abstract	Experiments were carried out using pin-on-disc tester in conformal lubricated contact conditions for different normal loads. Surface texturing was done using abrasive jet machining with the application of laser cut mask. In order to eliminate the effect of different input variables in all the experiments, pit-area ratio and sizes of oil pockets were very similar. Five types of oil pocket arrays were tested: radial, concentric, spiral, of a square arrangement, and of a random arrangement for 5% and 17% of pit-area ratio. Different dimple diameters caused various oil pocket densities. The experiments were also made for untextured polished discs. During tests, the friction force was monitored as a function of time. Before and after tests, disc surface topography was measured using a white light interferometer Talysurf CCI Lite. The beneficial effect of surface texturing was obtained for spiral arrays of dimples on disc surface. The presence of a radial array of oil pockets resulted in the worst tribological properties of tribological assemblies containing textured discs.
Słowa kluczowe:	teksturowane powierzchnie, tester trzpień-tarcza, siła tarcia, obróbka strumieniowo-ścierna.
Streszczenie	Badania przeprowadzono z wykorzystaniem testera tribologicznego typu trzpień-tarcza w warunkach styku rozłożonego, a ich celem było wykazanie zmian współczynnika tarcia wynikających z różnego szyku kieszeni smarowych. Węzeł cierny składał się z teksturowanej próbki (tarczy) i nietekstorowanej przeciwpróbki. Przeciwpróbka w celu zapewnienia styku rozłożonego mocowana była wahliwie na ramieniu pomiarowym urządzenia. Badania przeprowadzane były w warunkach ubogiego smarowania z wykorzystaniem typowego oleju maszynowego L-AN-46. Prędkość poślizgu, promień tarcia oraz ilość oleju podawanego w miejscu styku były stałe, zmieniano natomiast obciążenie normalne. Przedmiotem badań były tekstury wykonane w 5 szykach: spiralnym, promieniowym, koncentrycznym, kwadratowym i losowym. Przed i po badaniach mierzono topografię powierzchni próbek przy pomocy interferometru światła białego Talysurf CCI Lite. Wykazano, że szyk kieszeni smarowych przy tym samym stopniu pokrycia i głębokości tekstury ma wpływ na wartości współczynnika tarcia.

INTRODUCTION

The introduction of specific textures on sliding surfaces, including micropits (or holes, dimples, cavities, oil pockets) is an approach to improve the seizure resistance of sliding elements **[L. 1]**. Those micropits may reduce friction by acting as reservoirs for lubricant. Holes can also serve as micro-traps for wear debris in lubricated or dry sliding. Perhaps the plateau-honing was the first example of surface texturing **[L. 2]**. Various techniques can be employed for surface texturing including machining, ion beam texturing, etching, and laser texturing **[L. 3]**. Laser texturing is the most popular technique **[L. 4]**. However, abrasive jet machining is a promising method **[L. 5, 6]**.

Surface texturing was shown to provide tribological benefits in terms of friction reduction in conformal contact. Many experiments have been performed using pin-on-disc testers **[L. 7, 8, 9]**. Kovalchenko et al. **[L. 7]** found that the presence of dimples increased the range of hydrodynamic lubrication. Surface texturing of the disc caused an improvement of seizure resistance of a sliding pair made of cast iron **[L. 8]**. Friction tests were carried out using a pin-on-disc friction machine in a unidirectional sliding motion **[L. 9]**. The results showed that the textured surfaces exhibited a lower friction coefficient and wear compared with the untextured topographies. On the basis of literature review, it is possible to select parameters of textured surfaces like pit-area ratio (oil pockets density), dimple

---

[*] Rzeszow University of Technology, 35-959 Rzeszow, Al. Powstańców Warszawy 12, Poland.

depth, width, and surface roughness in areas free of dimples [L. 1, 3]. However, the effect of the pattern of oil pockets on tribological behaviour of sliding elements has not been fully explained. It is usually selected based on the intuition of researchers. There are only a few publications in this field. Dimples evenly distributed as a square or hexagonal array are the normal arrays. The tribological performance of graphene nanosheets as oil additives on surfaces with a square pattern of dimples was investigated. The oil with additives showed good tribological properties, particularly on the textured surfaces, and a wear reduction of over 90% was achieved [L. 10]. However, oil pockets can also be randomly distributed. Random arrangement of dimples on cylinder liner surfaces caused a decrease in friction force of about 50% in a fluid lubrication regime, compared to untextured samples [L. 11]. The pattern containing both large and small dimples was described in [L. 12]. The load-carrying capacity was obviously improved compared with both patterns with only large or small oil pockets. The authors of papers [L. 13, 14] discussed the effect of multi-shape surface texturing on tribological properties in flat-on-flat contact. The beneficial effect of textured surfaces was more evident at higher sliding speeds.

In order to increase seizure resistance, the contact between surfaces should be interrupted by the presence of dimples, this requirement affects oil pocket arrays [L. 15].

Optimisation of oil pocket patterns is an approach to enhance the tribological effect on the whole surface, because two adjacent dimples would have interactions with each other. By shifting the lines of the dimples, oil pocket columns would be at an angle of α to the line of the dimples with the same pit-area ratio. It was found that hydrodynamic pressure could be increased up to 22% by optimizing α angle [L. 16]. Researchers [L. 17] proposed a novel phyllotactic pattern for dimple positioning in the internal surface of journal bearings. It was shown that the frictional coefficient of bearings with a phyllotactic pattern of oil pockets was lower than that with linear (squared) array. A phyllotactic array was also applied to thrust bearing surfaces. It presented a better lubrication effect than radial and malposed patterns [L. 18].

In this work, an attempt was made in order to explain the mechanism of the influence of selected oil pocket patterns on the tribological properties of contacting elements.

EXPERIMENTAL DETAILS

Experiments were carried out using a pin-on disc tester. Different types of steel discs from 42CrMo4 material of 50 HRC hardness with a diameter of 25.4 mm were tested in unidirectional sliding under starved lubricated conformal contact conditions. During tests, the friction force was monitored as a function of time. The friction force was measured by extensometer sensor made by the Hottinger Company of type S2 with a measurement range

up to 50 N and an accuracy class of 0.1. Tribological tests were carried out in an ambient temperature of 23ºC. Revolving speed was controlled by an inductive position transducer, type SCID-1 ZVN. All tests were carried out at the same sliding speed of 0.4 m/s and number of revolutions (10000). Normal loads were 20 N, 40 N, and 60 N. Each test was repeated 3 times. New samples were used for each repetition.

Before tests, the co-acting surfaces of discs were polished and then textured using abrasive jet machining. Texture patterns were obtained with the use of laser-cut masks made of glass-fibre strengthen engraving foil. Five types of oil pockets arrays were tested: radial, concentric, spiral, of a square arrangement, and of a random arrangement – see **Figs. 1** and **2**. The reference polished sample was also tested. Discs co-acted with a self-aligned small disc of 5 mm diameter with a chamfering of 0.5 mm x 45° sizes, made from 42CrMo4 steel also of 50 HRC hardness, fixed by a specially made pin. Contact surfaces of the small disc were also polished. This construction was used to ensure conformal contact between lubricated surfaces. It was applied in the previous works of the present authors [L. 19, 20]. The centres of the small disc were positioned at contact track radius of 8 mm.
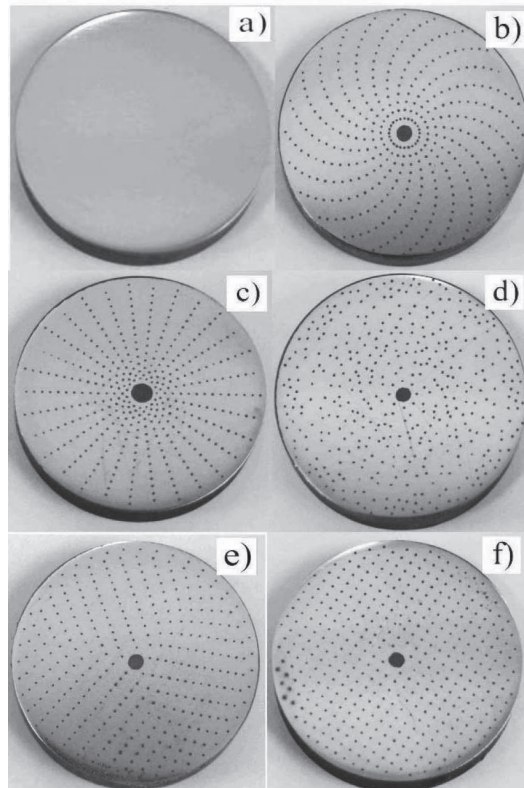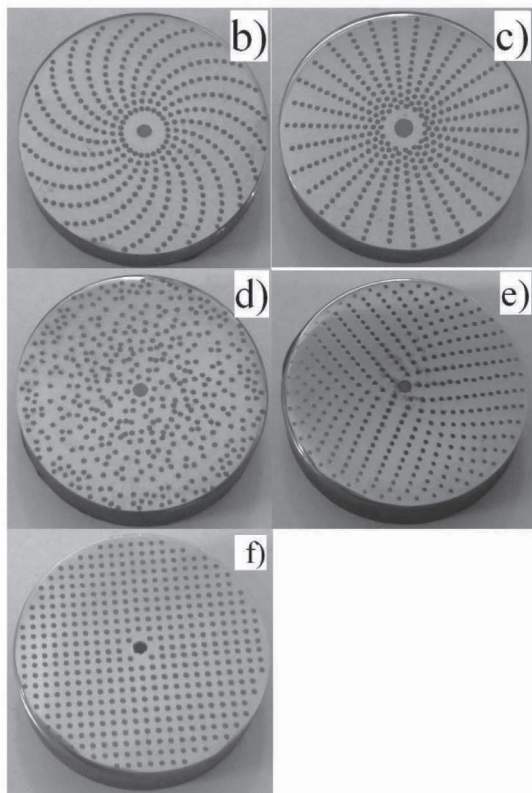

Fig. 1. **Tested discs with a pit-area ratio of 5%: a) untextured, b) with spiral rows array, c) with radial rows array, d) with random array, e) with concentric array, f) with square array**

Rys. 1. Testowane tarcze ze stopniem pokrycia 5%: a) nie-teksturowany dysk, b) układ spiralny, c) układ pro-mieniowy, d) układ losowy, e) układ koncentryczny, f) układ kwadratowy

One drop of oil L-AN-46 (kinematic viscosity in 400C 46.0 mm²/s, in 1000C 6.66 mm²/s, viscosity index 96, ignition temperature min. 1700C, flow temperature max. -120C, density in 150C 880 kg/m³) was supplied into the inlet side of the contact zone before each test. No additional amount of oil was added during test. It was found that one drop of oil was sufficient for filling all dimples on textured discs. Before tests, discs samples were measured by a Talysurf CCI Lite white light interferometer. Arrays of dimples were made to ensure a constant density of 5% and 17% in contact area. Diameters of holes were 0.2–0.25 mm for a pit area ratio of 5% and 0.5–0.55 mm for an oil pocket density of 17%, while their depths varied from 8 to 10 µm. Spiral rows on textured disc (**Figures 1b** and **2b**) were equally spaced; the number of dimples on disc circumference was 24, and the angle between rows was 15º. Radial rows of oil pockets (**Figures 1c** and **2c**) were obtained with an angle between rows of 12º and radial spacing between dimples centres of 0.8 mm. Discs shown in **Figures 1d** and **2d** were obtained by randomly putting dimples on contact track area to ensure the correct pit-area ratio. Discs with concentric patterns (**Figures 1e** and **2e**) were made by putting dimples at the circumference of theoretical circle (each next circle diameter was larger by 1.6 mm) with a constant spacing 1.7 mm between dimples.

Fig. 2.   Tested discs with a pit-area ratio of 17%: b) with spiral rows array, c) with radial rows array, d) with random array, e) with concentric array, f) with square array

Rys. 2.   Testowane tarcze ze stopniem pokrycia 17%: b) układ spiralny, c) układ promieniowy, d) układ losowy, e) układ koncentryczny, f) układ kwadratowy
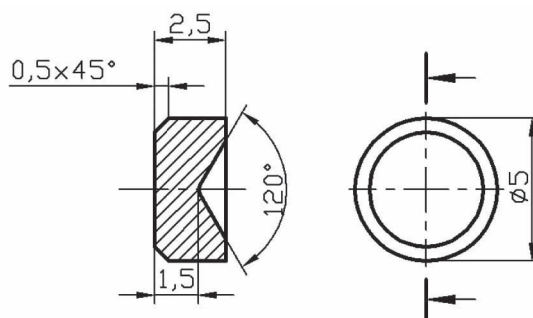
Fig. 3.   Small disc with dimensions
Rys. 3.   Przeciwpróbka wraz z wymiarami

Disc with a square pattern of oil pockets ensured an equal spacing between dimples of 1.05 mm. **Figures 4** and **5** present contour plots of tested disc surfaces. After texturing, the pile-ups were removed by substantial polishing. The surface roughness of the textured discs in the areas free of oil pockets, the untextured disc, and the small disc determined by the Ra parameter was 0.06 µm. **Figures 6** and **7** present examples of profiles containing dimples.
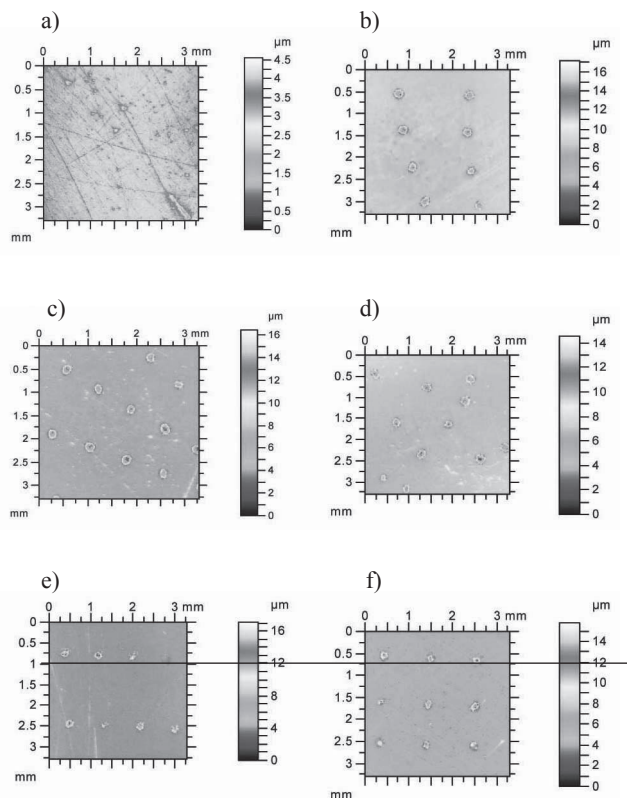
Fig. 4.   Contour plots of surfaces from tested discs: a) untextured b) with spiral rows array, pit-area ratio of 5%, c) with radial rows array, pit-area ratio of 5%, d) with random array, pit-area ratio of 5%, e)with concentric array, pit-area ratio of 5%

Rys. 4.   Profile powierzchni testowanych dysków: a) nietekstu-rowany, b) szyk spiralny, stopień pokrycia 5%, c) szyk promieniowy, stopień pokrycia 5%, d) układ losowy, stopień pokrycia 5%, e) szyk koncentryczny, stopień pokrycia 5%, f) szyk kwadratowy, stopień pokrycia 5%
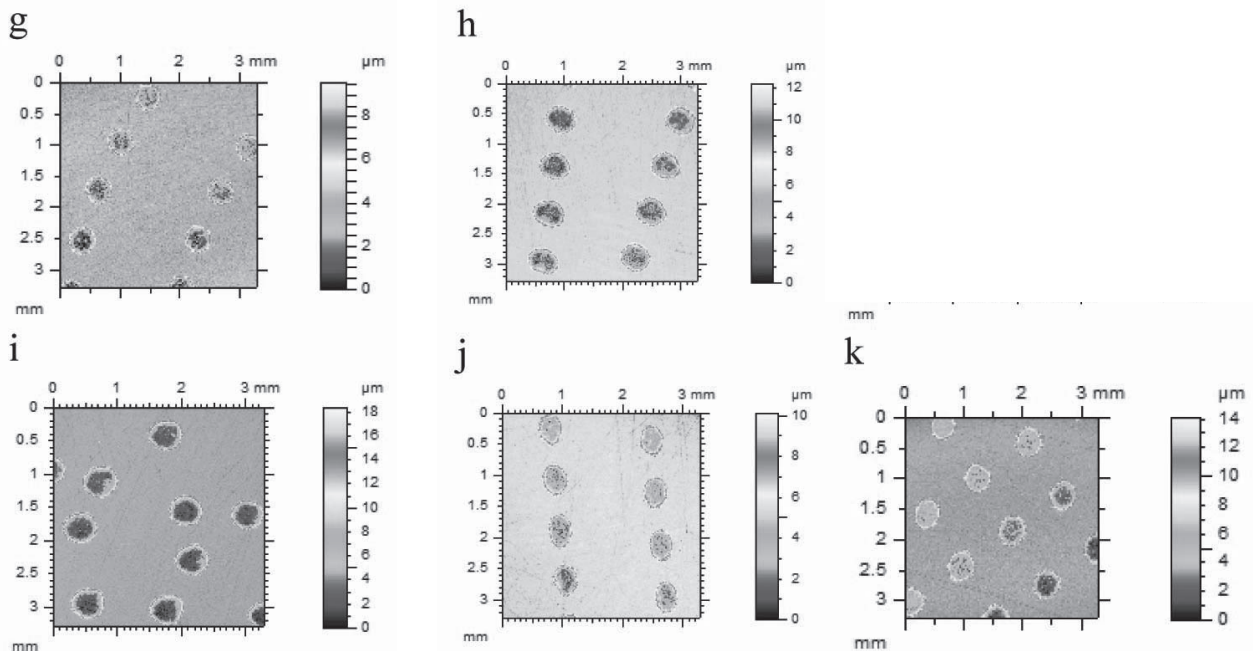
Fig. 5. **Contour plots of surfaces from textured discs with pit-area ratio of 17%: a) with spiral rows array, b) with radial rows array, c) with random array, d) with concentric array, e) with square array**

Rys. 5. Profile powierzchni testowanych dysków przy stopniu pokrycia 17%: a) szyk spiralny b) szyk promieniowy, c) układ losowy, stopień pokrycia 17%, d) szyk koncentryczny, stopień pokrycia 17%, e) szyk kwadratowy, stopień pokrycia 17%
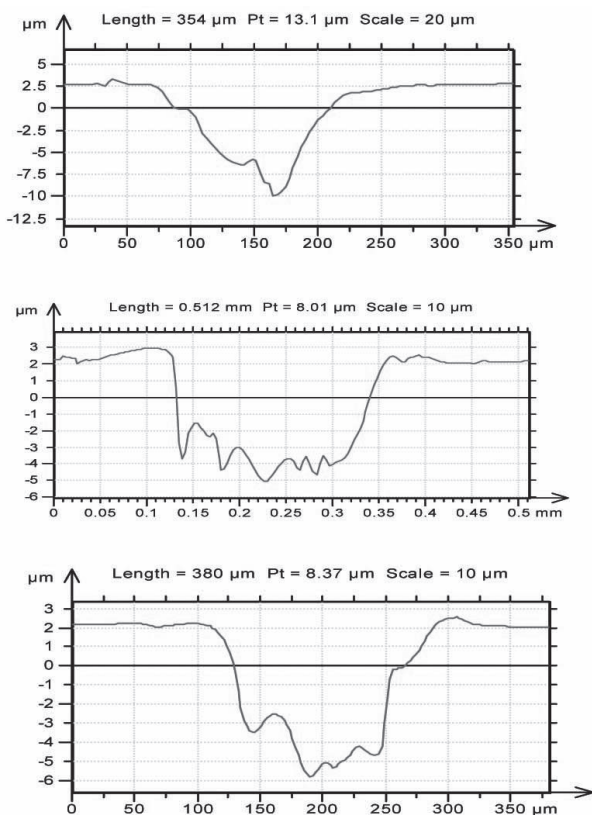
Fig. 6. **Profiles of textured surfaces for a pit-area ratio of 5%**

Rys. 6. Wybrane profile chropowatości teksturowanych powierzchni dla stopnia pokrycia 5%
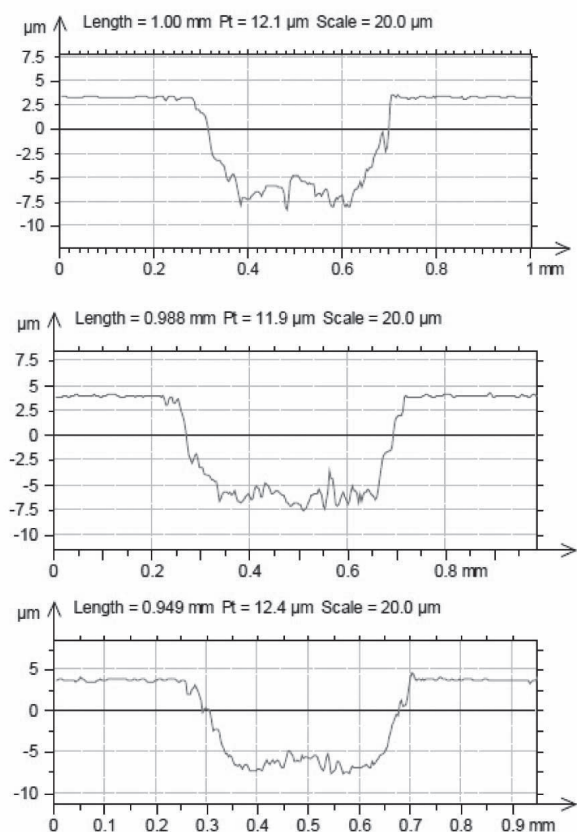
Fig. 7. **Profiles of textured surfaces for a pit-area ratio of 17%**

Rys. 7. Wybrane profile chropowatości teksturowanych powierzchni dla stopnia pokrycia 17%

RESULTS AND DISCUSSION

Figures 8, 9, and **10** show examples of the variation of friction force with the number of revolutions for sliding pairs with textured and untextured discs for normal loads of 20, 40, and 60 N, respectively. Table 1 presents the average, minimum, and maximum values of the coefficient of friction for all test repetitions. The coefficient of friction was calculated as the ratio of the friction force to the normal force.

For the smallest load (20 N) and pit-area ratio of 5%, the friction force initially abruptly increased, obtained the maximum value, decreased, and slowly increased (**Figure 8**). For the untextured sample, fluctuations were found with individual peaks visible on the friction force curve. In these conditions, the behaviours of sliding pairs with textured discs were typically better than those with untextured discs. The average values of the coefficient of friction of assemblies with textured samples were smaller than with polished disc. For disc with radial patterns of dimples, the mean coefficient of friction was similar to that of untextured disc. Significant variations were found in repetitions of tests with untextured disc. In this case, the smallest and the highest values of the coefficient of friction from all of the tested sliding pairs were obtained: 0.018 and 0.025, respectively. The scatter of the coefficient of friction was 0.007. Dispersion of the friction coefficient of the sample with radial rows of oil pockets was also large (0.006) for samples with a pit-area ratio of 5%. For the other cases, dispersion was comparatively low (0.002 – 0.003). Generally, the tendency was observed that low mean values corresponded to low scatters of the coefficient of friction. The smallest average values and the smallest spreads of the friction force were found for the spiral array of oil pockets. In this case, the mean value of the coefficient of friction decreased about 10% compared to an untextured disc.

Better friction reduction due to surface texturing was obtained for a higher density of oil pockets. For the smallest load (20 N) and pit-area ratio of 17%, the friction force started from a low value and then increased (**Figure 8**). The smallest coefficient of friction was obtained for the assembly with the spiral disc (0.012). The lowest value of the coefficient of friction corresponded to the smallest scatter of the friction force (0.003). In this case, a decrease in the friction force was comparatively high (43%) compared to the untextured disc sample. Surface texturing also led to a decrease in the coefficient of friction for random and square arraies (about 10%). In only one case (concentric square), the surface textures caused an increase in the friction force (16%) compared to the polished disc sample.

Generally, for the smallest normal load, the increase of pit ratio led to an increase of the variation of the coefficient of friction. The highest scatter (0.021) of the friction coefficient was obtained for the sliding pair

Fig. 8. Variation of friction force with the number of revolution for sliding pairs with textured samples for pit-ratios of 5% and 17%; normal load was 20 N

Rys. 8. Wykresy siły tarcia w odniesieniu do liczby obrotów dla teksturowanych par ciernych przy stopniu pokrycia 5% i 17%; siła normalna 20 N

Fig. 9. Variation of friction force with the number of revolution for sliding pairs with textured samples for pit-ratios of 5% and 17%; normal load was 40 N

Rys. 9. Wykresy siły tarcia w odniesieniu do liczby obrotów dla teksturowanych par ciernych przy stopniu pokrycia 5% i 17%; siła normalna 40 N
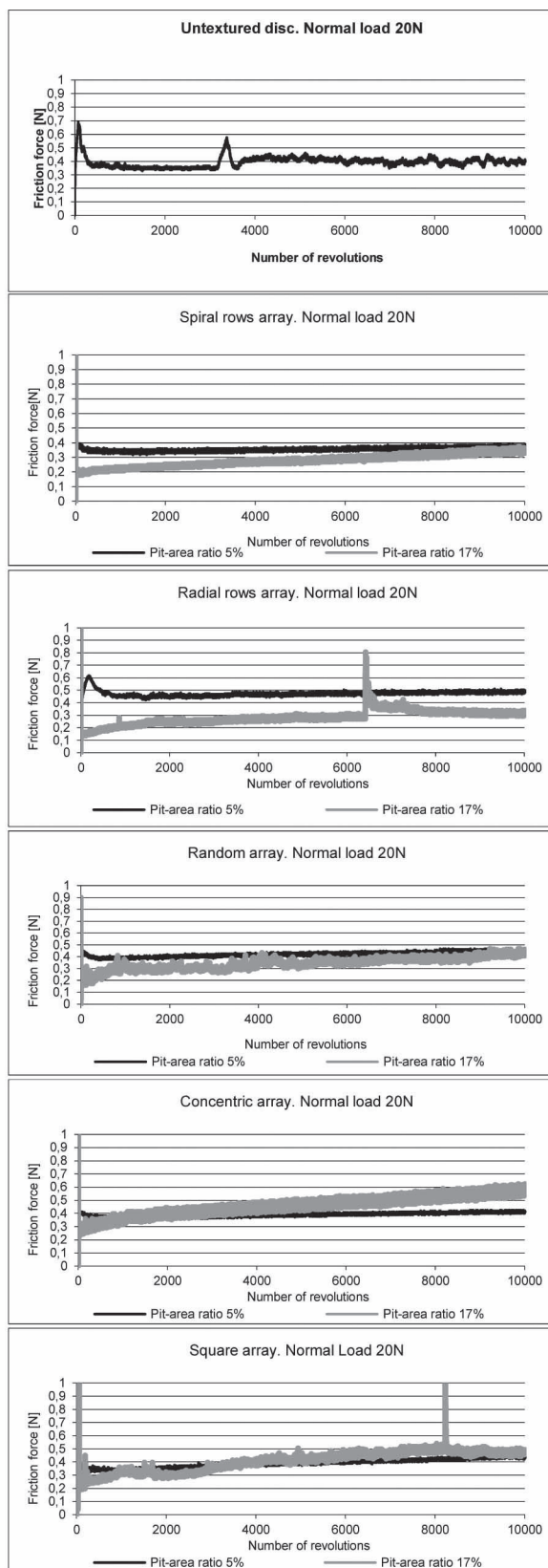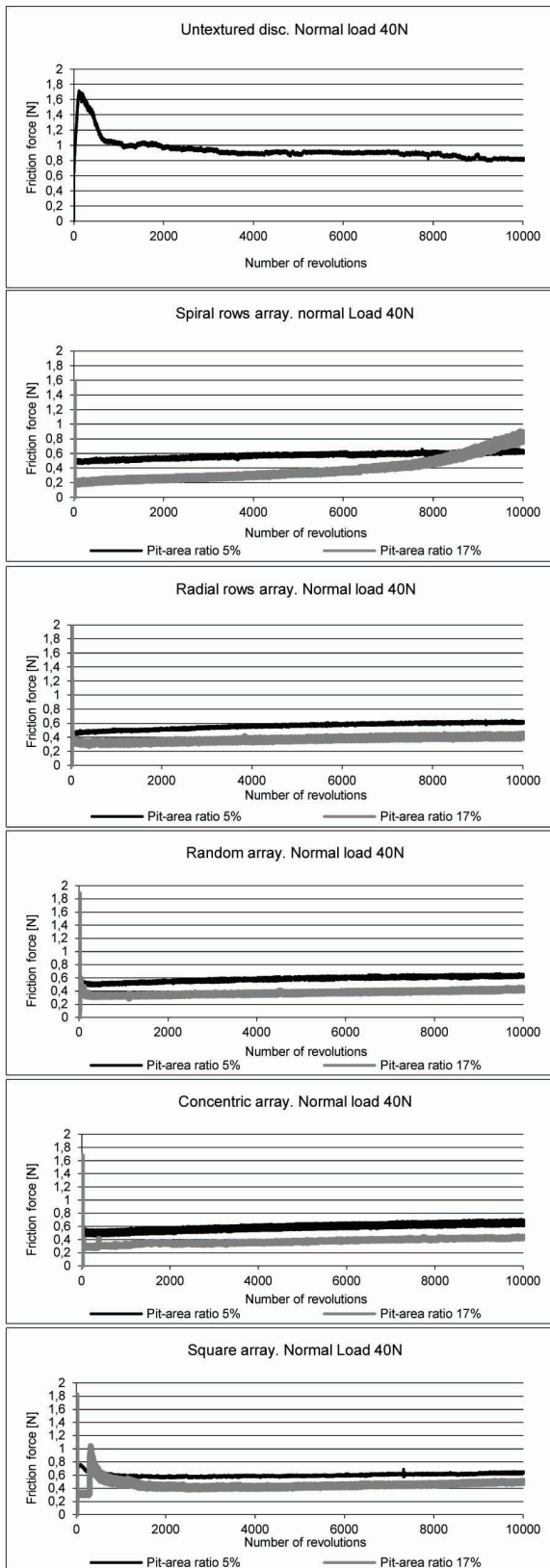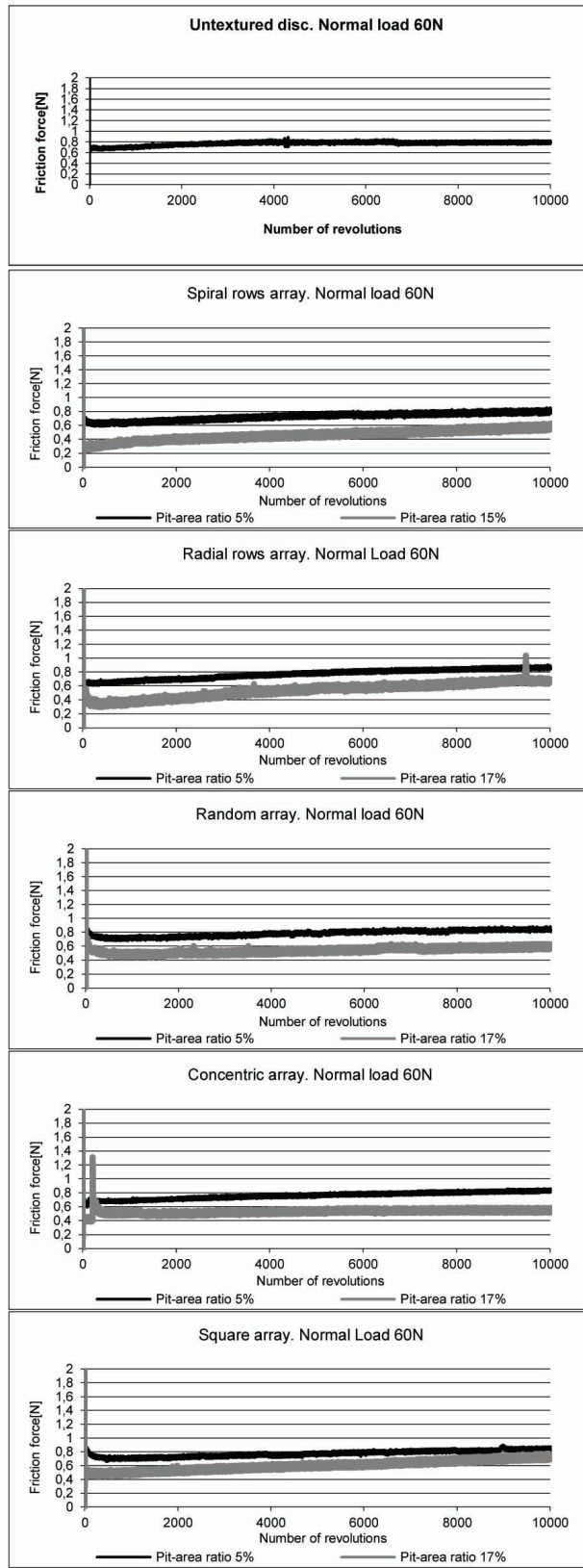

Fig. 10. Variation of friction force with the number of revolution for sliding pairs with textured samples for pit-ratios of 5% and 17%; normal load was 60 N

Rys. 10. Wykresy siły tarcia w odniesieniu do liczby obrotów dla teksturowanych par ciernych przy stopniu pokrycia 5% i 17%; siła normalna 60 N

Table 1.   **Average values of the coefficient of friction**
Tabela 1. Średnie wartości współczynnika tarcia

Disc type / Normal load		Untextured disc Spiral array	Pit ratio 5%					Pit ratio 17%				
			Radial rows array	Random array	Concentric array	Square array	Spiral array	Radial rows array	Random array	Concentric array	Square array	
		Friction coefficients										
20N	Max.	0.025	0.020	0.024	0.023	0.022	0.022	0.013	0.033	0.024	0.028	0.022
20N	Min.	0.018	0.018	0.018	0.020	0.019	0.019	0.010	0.012	0.015	0.023	0.013
20N	Average	0.021	0.019	0.021	0.021	0.020	0.020	0.012	0.022	0.019	0.025	0.019
40N	Max.	0.020	0.018	0.018	0.017	0.017	0.017	0.012	0.012	0.010	0.010	0.012
40N	Min.	0.015	0.015	0.015	0.014	0.016	0.015	0.009	0.008	0.008	0.009	0.009
40N	Average	0.018	0.017	0.017	0.015	0.016	0.016	0.011	0.010	0.009	0.009	0.011
60N	Max.	0.014	0.014	0.015	0.014	0.015	0.016	0.009	0.018	0.012	0.013	0.013
60N	Min.	0.013	0.013	0.013	0.013	0.013	0.014	0.008	0.009	0.009	0.009	0.009
60N	Average	0.014	0.013	0.014	0.013	0.014	0.015	0.008	0.013	0.010	0.010	0.011

with a radial array of oil pockets. For the other cases, the scatter was in the range of 0.005–0.009.

An increase of load from 20 N to 40 N caused a decrease in the coefficient of friction (see **Table 1**). For the middle normal load (see **Figure 9**) for sliding pairs with textured surfaces, the friction force after initial changes was stable or slowly increased. Behaviour of the sliding pair with untextured discs was different; the friction force obtained a high value (1.7 N) and then decreased. Under these conditions, disc surface texturing for a pit-area ratio of 5% resulted in a decrease in the frictional resistance up to 17%. However, contrary to the smallest load, performances of sliding pairs with various dimple patterns were similar to each other. The smallest coefficient of friction was obtained for the random array of oil pockets. Large fluctuations of the friction force for untextured discs were confirmed. Similar to the smallest load, the scatter of the coefficient of friction was high – 0.005. Dispersion of the coefficient of friction for textured samples was much smaller (between 0.001 and 0.003), and square and concentric patterns gave smaller spreads.

Surface texturing with a pit-area ratio of 17% caused a decrease in the coefficient of friction between 1.6 and 2 times for the medium normal load. Similar to the lower density of dimples, the lowest scatter of the friction force was obtained for concentric and random arrays (0.001–0.002), while the highest was for a radial layout (0.004).

Generally, for the middle normal load, surface texturing caused decreases in friction force mean values and the spread independent of dimple patterns.

When the highest normal load was applied, the smallest values of the coefficient of friction were obtained. The friction force, after reaching a maximum value and decreasing slowly, increased independently of disc type (see **Figure 10**). For the sliding pair with the untextured disc sample, the scatter of the coefficient of friction was low (0.001). Also scatters of the coefficient of friction were small for assemblies with textured samples of smaller pit density (between 0.001 and 0.002). Dispersion of frictional resistance was smaller compared to smaller loads. Low friction force scattering of the sliding pair with untextured discs deserves attention. The smallest spread of the coefficient of friction was obtained for spiral and random dimples patterns (0.001). For the highest load, the effect of texturing on the improvement of tribological behaviour of sliding elements was small for the pit ratio of 5% to 7.5% for spiral and 6.8% for concentric pattern of dimples.

Surface texturing caused a decrease in the coefficient of friction for larger dimple densities and the highest normal load. The highest reduction in the frictional resistance (about 43%) was achieved for the assembly with a spiral array of dimples compared to the sliding pair with the untextured sample. In this case, the variation of the friction force was also small. The highest coefficient of friction value and spread was found for the radial row sample (0.013 and 0.09, respectively). For the other cases, the mean values and the scatters of the friction coefficient were 0.01–0.011 and 0.003–0.004, respectively.

Due to high hardness of contacting elements, their wear was negligible.

DISCUSSION

Growth in the normal load led to a decrease in the coefficient of friction. A similar behaviour was found in the other research, for example, in **[L. 19]**.

In most cases, the friction force slowly increased in middle and final parts of tests. This increase was probably caused by the decrease in the amount of oil on disc's surface as tests progressed.

The effect of oil pocket patterns on the frictional resistance of the analysed sliding pairs was evident for the smallest applied load of 20 N. Introduction of surface texturing typically caused a decrease in the mean values of the coefficient of friction up to 43% as well as a decrease in data spreads. Only in one case (concentric array, pit-area ratio of 17%) did surface texturing lead to an increase in the coefficient of friction. From among assemblies with textured discs, the best results were obtained for a spiral pattern of dimples (low mean value and the smallest scatter of the friction force) independent of the density of dimples; however, the worst results were found for the array with radial rows (the big average value and the highest spread of the friction force). For the medium load of 40 N, the beneficial effect of surface texturing was evident for all analysed textured surfaces, the mean coefficient of friction decreased up to 49.5%, and its scatter decreased up to 5 times compared to untextured discs. Under medium load, the beneficial effect of disc surface texturing was independent of the dimple pattern for both pit-area ratios.

When the highest normal load of 60 N was applied, to samples with small oil pocket densities, the effect of surface texturing on the decrease in the coefficient of friction was small – its mean value decreased up to 7.5%. An increase in the normal load from 40 to 60 N caused a considerable decrease in the coefficient of friction scattering for the assembly with untextured discs (about 5 times). As a result, the friction force spreads were similar for pairs with textured discs and the majority of untextured discs. However, a different situation took place for assemblies with higher oil pocket densities. In this case, the smallest values and spreads were obtained for sliding pairs with spiral patterns, but the highest values were with radial patterns.

For the smallest and medium normal loads, the scatter of the coefficient of friction for test repetitions decreased due to surface texturing. The lack of oil containers on the untextured surfaces probably caused friction force variations. In this case, in initial test portions, there was probably a problem with creating convergent lubricating film, and a lubricant was squeezed from co-acted surfaces, and fluid friction was transformed into boundary or mixed friction. This problem is important for small loads, but it became negligible when the highest load was applied.

The beneficial effect of surface texturing was visible for higher pit-area ratios (for smaller dimples density this effect was marginal). The influence of the oil pocket arrays on the tribological performance of sliding elements was the highest for the smallest normal load. Change from the concentric array to the spiral layout caused a reduction in the coefficient of friction of more than twofold. The effect of dimple arrays was also visible for the highest load.

The positive effect of surface texturing was obtained for spiral arrays of dimples on the disc surface. Both small values and scattering of the friction force of the assembly with a spiral array of oil pockets were probably caused by the uniform contact between small disc and dimples. The presence of a radial array of oil pockets resulted in the worst tribological properties of tribological assemblies containing textured discs. For a radial array of dimples, the number of oil pockets in the contact area varied more than the other textured surfaces. The non-stable number of dimples in the contact area could cause instability in hydrodynamic lift generated by dimples. Frictional performance can be also attributed to the lubrication compensation of the neighbouring oil pockets. For radial patterns, a free region existed. The best compensation was possible for dimples with a spiral pattern. This layout is similar to the phyllotactic pattern of good performance **[L. 18]**. The tribological performance of the assembly with a spiral pattern of dimples was better than that with radial oil pocket arrays for an area density of 17% **[L. 20, 21]**.

Compared to the radial pattern, tribological behaviour was also improved after introducing other arrays of dimples.

CONCLUSIONS

The presence of dimples created by abrasive jet machining on disc surfaces typically resulted in a decrease in the coefficient of friction compared to polished disc textures in conformal contact conditions for all used normal loads. However, this effect was substantial for higher pit-area ratios (up to 50) and marginal for smaller oil pocket densities (lower than 20%). Low oil pocket densities are useful to achieve higher stability of the friction coefficient independently of normal load. High oil pocket densities may be connected with greater fluctuation in the friction force; however, for all used normal loads, a reduction in the coefficient of friction over 40% was achieved.

The effect of dimple pattern was visible mainly for the smallest load of 20 N. For higher pit-area ratios, the change from the concentric layout to the spiral array led to a reduction in the coefficient of friction more than twofold.

For the medium load of 40 N, the surface texturing resulted in a decrease in the coefficient of friction between 17% (low dimples density) and 49.5% (high pit-area ratio) compared to untextured samples. Under

this condition, the largest fluctuation of the coefficient of friction was obtained for polished discs. However, the effect of dimple patterns on the friction reduction was marginal.

When normal load was the largest (60 N), the effect of surface texturing on the improvement of the sliding properties of the analysed assembly was negligible for a pit ratio of 5%. However, for a dimple density of 17%, a significant reduction in the friction force (over 40%) was observed. The smallest spread of the friction force was achieved for the spiral pattern of oil pockets.

The radial pattern of oil pockets led to the worst tribological properties of tribological assemblies containing textured discs. In this case, the mean values and dispersions of the friction force were high. The best effect of surface texturing on tribological properties of sliding elements was obtained for spiral arrays of dimples on disc surfaces, and both small values and scattering of friction force were achieved. The other arrays of dimples (concentric, array, and square) assured typically better properties than the radial pattern and worse than the spiral layout.

REFERENCES

1. Nilsson B., Rosen B-G., Thomas TR et al.: Oil pockets and surface topography: mechanism of friction reduction. XI International Colloquium on Surfaces. Chemnitz (Germany) 2004. Addendum.
2. Pawlus P.: Effects of honed cylinder surface topography on the wear of piston-piston ring-cylinder assembly under artificially increased dustiness conditions. Tribology International 1993; 26: 49–55.
3. Etsion I.: State of the art in laser surface texturing. Proceedings of the 12th Conference on Metrology and Properties of Engineering Surfaces. Rzeszów (Poland) 2009: 17–20.
4. Etsion I.: Improving tribological performance of mechanical components by laser surface texturing. Tribology Letters 2004; 17: 733–737.
5. Wakuda M., Yamauchi Y., Kanzaki S. et al.: Effect of surface texturing on friction reduction between ceramic and steel materials under lubricated sliding contact. Wear 2003; 254: 356–363.
6. Nakano M., Korenaga M., Miyake K. et al.: Applying micro-texture to cast iron surfaces to reduce the friction coefficient under lubricated conditions. Tribology Letters 2007; 28: 131–138.
7. Kovalchenko A., Ajayi O., Erdemir A. et al.: The effect of laser surface texturing on transitions in lubrication regimes during unidirectional sliding contact. Tribology International 2005; 38: 219–225.
8. Mishra S.P. and Polycarpou A.A.: Tribological studies of unpolished laser surface textures under starved lubrication conditions for use in air-conditioning and refrigeration compressors. Tribology International (in press).
9. Hu T., Hu L. and Ding Q.: The effect of laser texturing on the tribological behaviour of Ti-6Al-4V. Proc. IMechE. Part J: Journal of Engineering Tribology 2012; 226: 854–863.
10. Zheng D., Cai Z-B., Shen M-X el al.: Investigation of the tribology behaviour of the graphene nanosheets as oil additives on textured alloy cast iron surface. Applied Surface Science 2016; 387: 66–75.
11. Grabon W., Koszela W., Pawlus P. et al.: Improving tribological behaviour of piston ring–cylinder liner frictional pair by liner surface texturing. Tribology International 2013; 61:102–108.
12. Wang X.L., Adachi K., Otsuka K. et al.: Optimization of the surface texture for silicon carbide sliding in water. Applied Surface Science 2006; 253: 1282–1286.
13. Segu D.Z., Hwang P.: Friction control by multi-shape textured surface under pin-on-disc test. Tribology International 2015; 91: 111–117.
14. Segu. D.Z., Choi S.G., Choi J.H. et al.: The effect of multi-scale laser textured surface on lubrication regime. Applied Surface Science 2013; 270: 58–63.
15. Galda L., Dzierwa A., Sep J. et al.: The effect of oil pockets shape and distribution on seizure resistance in lubricated sliding. Tribology Letters 2010; 37: 301–311.
16. Yu H., Huang W., Wang X.: Dimple patterns design for different circumstances. Lubrication Science 2013; 25: 67–78.
17. Lu Y.S., Liu Y.M., Wang J. et al.: Experimental investigation into friction performance of dimples journal bearing with phyllotactic pattern. Tribology Letters 2014; 55: 271–278.
18. Lu Y.S., Liu Y.M., Wang J. et al.: Tribological performance with dimpled thrust bearings with phyllotactic pattern. Wear 2016; 346–347: 108–115.
19. Grabon W., Pawlus P., Wos S., Koszela W,, Wieczorowski M.: Effects of honed cylinder liner surface texture on tribological properties of piston ring-liner assembly in short time tests. Tribology International (in press).
20. Wos S., Koszela W., Pawlus P.: Tribological behaviours of textured surfaces under conformal and non-conformal starved lubricated contact conditions. Proc MechE Part J: Journal of Engineering Tribology 2015; 229: 398–409.
21. Wos S., Koszela W., Pawlus P.: Determination of oil demand for textured surfaces under conformal contact conditions. Tribology International 2015; 93: 602–613.